



A novel process to produce stratified structures in food

Anna Cäcilie Möller^a, Atze Jan van der Goot^{a,*}, Albert van der Padt^{a,b}

^a Food Process Engineering, Wageningen University, PO Box 17, 6700 AA, Wageningen, the Netherlands

^b FrieslandCampina, Stationsplein 4, 3818 LE, Amersfoort, the Netherlands

ARTICLE INFO

Keywords:

Continuity
Food structure
Anisotropy
Rheology
Processing
Stratification

ABSTRACT

A method to create stratified structures with static mixing elements initially developed for the plastic polymer industry is investigated here as a new route for structuring food dispersions. Food dispersions of different viscosities were structured with static mixing elements to investigate the potential of the method for foods. Differently coloured chocolates were used as the model products. The viscosity of the chocolate was controlled through the addition of pea fibre. The first step was the formation of 2–8 layers, with the two differently coloured chocolates. Then, the chocolate dispersions were layered into 256 layers with an approximate layer thickness of 60 µm. Layer formation was facilitated when using similar paste viscosity and when slip was induced through wall coating with vegetable oil. Uniaxial cutting tests of the layered chocolate indicated that layering resulted in different mechanical properties, parallel and perpendicular to the layers. Fibre orientation in the direction of flow was observed, resulting in the potential to induce anisotropy, additional to the layers. The higher viscous dispersions, wheat dough and melt cheese, could also be structured into layers, although the force constraints of the experimental set-up were reached. Mid-stream additions were added to produce strand structures instead of layers, resulting in higher hierarchy structures but less uniformity.

1. Introduction

Recently, renewed interest was shed on laminar mixing methods by which two or more fluids are extruded into layers that are stretched and folded on top of each other, respectively. The key element of this compounding process is a static mixer into which two or three fluid streams are fed in parallel, forming layers, due to the laminar flow conditions (at low Reynold numbers). This is in contrast to mixing processes in mixers that are based on turbulent fragmentation and reorientation of the volumes to be mixed. Similarly as in microfluidic processes, streams of fluid are directly controlled by the geometry of the device.

Such repetitive stretching and folding has been demonstrated for polymer melts but also for oil/water emulsions (Hofmann et al., 2021; Schaller et al., 2017). The application of laminar fractal mixing for food structuring has so far not been discussed. Natural food structures are heterogeneous, complex and mostly anisotropic. Structural and textural properties in food influence our perception and taste experience (Lillford, 2016). Therefore, methods to produce structures in foods are widely applied. Especially recently, efforts have been undertaken to copy existing product structures from novel raw materials to mimic 'traditional' foods, such as meat. These methods include extrusion and

3D printing (Nachal et al., 2019; Sandoval Murillo, Osen, Hiermaier and Ganzenmüller, 2019). Extrusion is widely applied in food production to obtain specific shapes and textures. Extrusion is still considered a complex process, due to the fact that multiple sections are highly linked through an interdependency of the process conditions and ingredient properties (Pietsch et al., 2018). Consequently, extrusion is still difficult to control. 3D food printing, usually extrusion based, offers the production of custom made foods (Liu et al., 2017), and flexible and rapid prototyping (Ma et al., 2021). So far the application of 3D printing for food is still limited by its scalability.

In this chapter, the potential of laminar fractal mixing is discussed and demonstrated for the structural design of food. In particular of multi-component food formulations. Laminar fractal mixing exploits the combination of different channel elements. These elements can be arranged differently, to design pre-defined structures according to controlled assembly and product requirements. As an example, layers can be continuously formed from macro to microscale. In bakery industry, laminar structuring could lead to process improvements, by avoiding dough weakening during common kneading processes (Cappelli et al., 2020; Muscalu et al., 2020). In other applications the method can lead to new flavour experiences, potentially by combining materials

* Corresponding author. Food Process Engineering, Wageningen University, PO Box 17, 6700 AA, Wageningen, the Netherlands

E-mail addresses: anna.moller@wur.nl (A.C. Möller), atzejan.vandergoot@wur.nl (A.J. van der Goot), albert.vanderpadt@wur.nl (A. van der Padt).

<https://doi.org/10.1016/j.jfoodeng.2023.111413>

Received 30 August 2022; Received in revised form 16 December 2022; Accepted 5 January 2023

Available online 23 January 2023

0260-8774/© 2023 The Authors. Published by Elsevier Ltd. This is an open access article under the CC BY license (<http://creativecommons.org/licenses/by/4.0/>).

of different texture and composition, i.e. a protein network and a fat phase. Furthermore, variation in taste, such as sweetness of the phases can be exploited for taste sensation. Stretching of fluid material in a channel can induce orientation of the components in the fluid. Orientation in fluid flow has been shown for fibre-like structures in polymer melts (Kugler et al., 2020), as well as for food polymers, i.e. caseins micelles during Mozzarella cheese production (McMahon et al., 1999), and could thus introduce additional anisotropy into the structures.

As the method is dependent on laminar flow conditions the material properties are important to ensure structure formation solely based on laminar flow in the channel geometry. Viscosity differences, normal stress differences or interfacial tension between the materials can induce distortions, making it less trivial to reach the intended structure (Neerinx et al., 2021). Furthermore, the smallest achievable domain size that can be obtained by this relatively easy compounding method is limited by the balance between the interfacial, inertial and viscous forces (Hofmann et al., 2021). This research aims to investigate the applicability of laminar fractal mixing to produce pre-defined structures with food materials. At first, the theory of the structuring method is reviewed, followed by an elaboration on its potential to produce anisotropic substructures. Then, first experiments are presented that describe the possibilities to form uniform layers and strands with food materials of different viscosities. Finally, the potential of laminar fractal mixing in food processing is discussed.

2. Theory

2.1. Principle of layer multiplication

Laminar fractal mixing is based on the baker's transformation. This operation received its name from dough kneading in the baking trade. It includes a stretching step of the material, whereafter the stream is either folded, or cut and stacked onto each other (Fig. 1).

Fractal mixers are static mixers, hence no parts of the mixer itself are moving. Within the mixers, the stream of stacked fluids is split, stretched and once again stacked onto each other, resulting in an exponential layer multiplication, upon repetition (Neerinx and Meijer, 2013). Fig. 1

demonstrates the fundamental steps of fractal mixing. Fluid volumes, here marked in black and white for the explanation, are stretched and then folded, or cut and stacked, to fill the size of the original volume element. Different channel designs were designed to enable this operation. Earlier designs included interface rotation steps (Appendix Figure A1) (Neerinx et al., 2011; Neerinx et al., 2011; Neerinx and Meijer, 2013; Schaller et al., 2017). These mixers were improved with the objective to optimise the regularity of the layering even after multiple repetitions of the operation. The rotating operations of the fluid stream (Appendix Figure A1) were in more recent developments avoided to minimize distortions of the structures (Neerinx et al., 2021). The optimized mixing scheme is depicted in Fig. 2. The focus of the design was to create a mostly straight flow channel. The first stretching in the direction of the flow is induced by a vertical compression step. The compression is subsequently reversed by a lateral extension, to return to

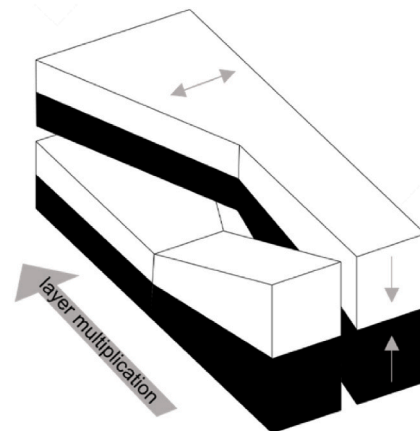


Fig. 2. Layer multiplication with converging and diverging channel adopted from (Neerinx et al., 2021), grey arrows indicate the vertical compression of the stream through the converging channel, and the lateral extension of the stream through the divergence of the channel.

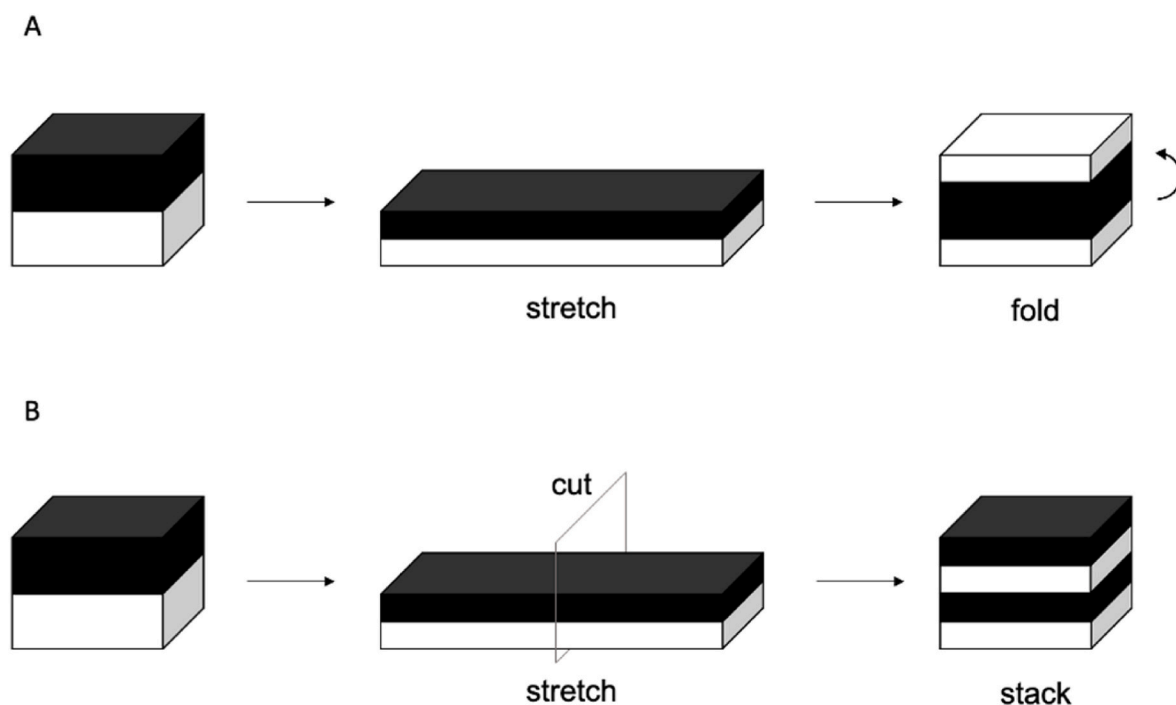


Fig. 1. Principle of the baker's transformation either by (A) stretching followed by folding, or (B) by stretching followed by cutting and stacking. Graphic adapted from (Schaller et al., 2017) with permission.

the original channel cross section. Thereby layering the volumes and avoiding interface rotation.

Further developments included the addition of layers oriented perpendicular to the initial layer surface (Fig. 4B and C). With subsequent layer multiplication the perpendicular layer addition increases the hierarchy of the structures. By repeating the layer additions and multiplication steps, higher hierarchy structures could be formed (Neerinx et al., 2021; Schaller et al., 2017).

Layer formation through laminar fractal mixing has been demonstrated to yield uniform structures of polymer melts, as well as of Nivea cream samples (Neerinx et al., 2021; Schaller et al., 2017). However, the formation of microstructures, in particular those with a more complex pattern resulted in less uniform structures. Even though the replacement of the rotation operation improved the uniformity of the hierarchical structures a lot (Neerinx et al., 2021), vertical stretching of horizontal layers still distorted the layers, comparable to previous results (Neerinx and Meijer, 2013).

So far, the method development and application of laminar fractal mixing was mainly focused on structural uniformity. The stacking has been shown to result in layer multiplication, stretching of the liquid stream caused layer thinning and served to maintain the continuity of the process (Hofmann et al., 2021; Schaller et al., 2017). We noted that the stretching step in this structuring process can have additional promising effects on the substructure of the different fluids in the stream, such as the orientation of the material in the flow direction. These effects have so far not been further described for laminar fractal mixing, and their potential benefits are therefore elaborated on in the following Section.

2.2. Stretching to induce fibre orientation in fluid flow

In a fluid, containing fibre-like components, a convergence of the channel induces extensional flow, which may result in orientation of these components in the direction of flow (Hsiao et al., 2017; Rivlin, 1948). Such fibre orientation could introduce an additional level of anisotropy in the substructure of the layers.

The latest laminar static mixer geometries include a short stretching step (Fig. 2), according to the baker's transformation. The stretch is induced by converging the channel geometry in the vertical direction. Accordingly, the convergence can induce extensional flow, which induces extensional stress on the fluid. In order for a fibre-like component or molecule to orient in a fluid flow, it needs to be exposed to the extensional flow for sufficient time or distance (Vincent and Agassant, 1985). Subsequent to stretching the material, the channel diverges into the horizontal direction (Fig. 2), which can result in decrease of the extensional stress. Materials can be constrained in the stretched conditions for a longer time and distance, by avoiding the channel divergence. Recombination of the stretched layers at the reduced channel cross section allows to keep the flow velocity constant after stretching (v_2), and maintain the extension on the fluid (Fig. 3). The iterative

decrease of the channel dimensions could be overcome by the addition of layers perpendicular to the original layers, and concurrently also increase the hierarchical structure of the material.

3. Experimental

3.1. Materials

Multiflux elements were drawn in SolidWorks Software (Dassault Systèmes SolidWorks Corp., France) according to the cutting-stretching-stacking design of (Neerinx et al., 2021) and processed in PreForm 3.22.1 (Formlabs Inc., USA) for 3D printing. The elements were 3D printed from Grey Resin V4 (Formlabs Inc., USA) on a Form 2 SLA 3D Printer (Formlabs Inc., USA) with a layer thickness of 0.16 mm.

Milk chocolate, dark chocolate and white chocolate (Delicata, Albert Heijn, The Netherlands), cheddar melt cheese (Cheddar Kaas, Jumbo, The Netherlands), wheat flour (Albert Heijn the Netherlands), and dill (Dille Vers, Jumbo, The Netherlands) were purchased from local supermarkets (Albert Heijn, the Netherlands; Jumbo, The Netherlands). Stained cocoa butter (white and black) was purchased online (Brand-NewCake, The Netherlands). Yellow pea fibre isolate was purchased from Roquette Frères S.A. (St. Louis, USA), sodium caseinate powder was kindly provided by FrieslandCampina (The Netherlands).

3.2. Chocolate preparation

The chocolates were melted in a water bath at 40 °C. Black and white stained chocolate samples were made by mixing 200 g chocolate (white or milk) with 15 g white or black stained cocoa butter, respectively. To adjust the viscosity of white and milk chocolate, 5 g yellow pea fibre isolate was added to the milk chocolate mix, and 15 g pea fibre isolate was added to the white chocolate mix to increase the viscosity of the dispersion. The chocolate mixes were placed back in the water bath and stirred until they reached 40 °C. The temperature was monitored with an electronic thermometer (VWR International, US).

3.3. Preparation of melt cheese and production of wheat dough

The cheddar melt cheese was tempered at 60 °C before the structuring experiments. 120 g wheat flour was mixed with 60 mL water and kneaded until a smooth dough was obtained. The dough was rested at 4 °C, overnight.

3.4. Structuring in static mixer

3.4.1. Chocolate structuring

The Multiflux elements were assembled into a structuring channel. For layer formation the channel was assembled with up to 7 splitting serpentine elements (Fig. 4A), an inlet and outlet part, and homogenizer elements ('H' and 'I'), placed before and after the splitting serpentine

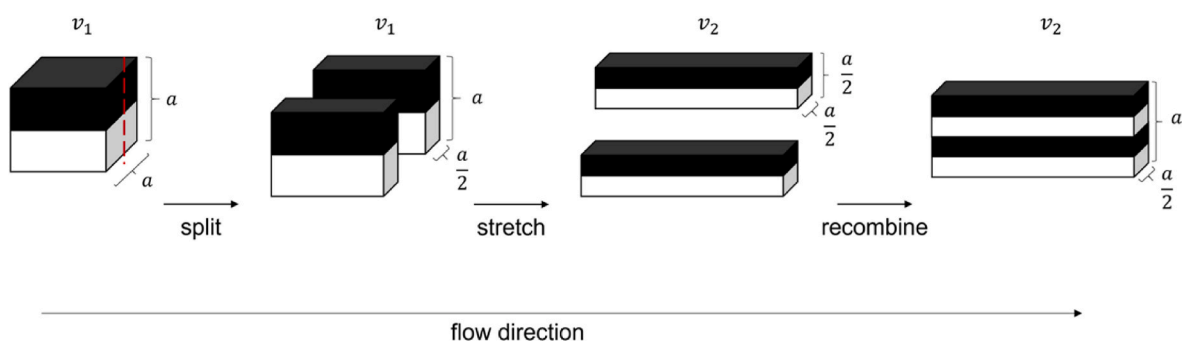


Fig. 3. Layer multiplication with stretch induced by vertical convergence to half of the channel cross section, with subsequent stream recombination to retain extensional stress on fluid. v_1 is the flow velocity before channel convergence, v_2 is the flow velocity after channel convergence.

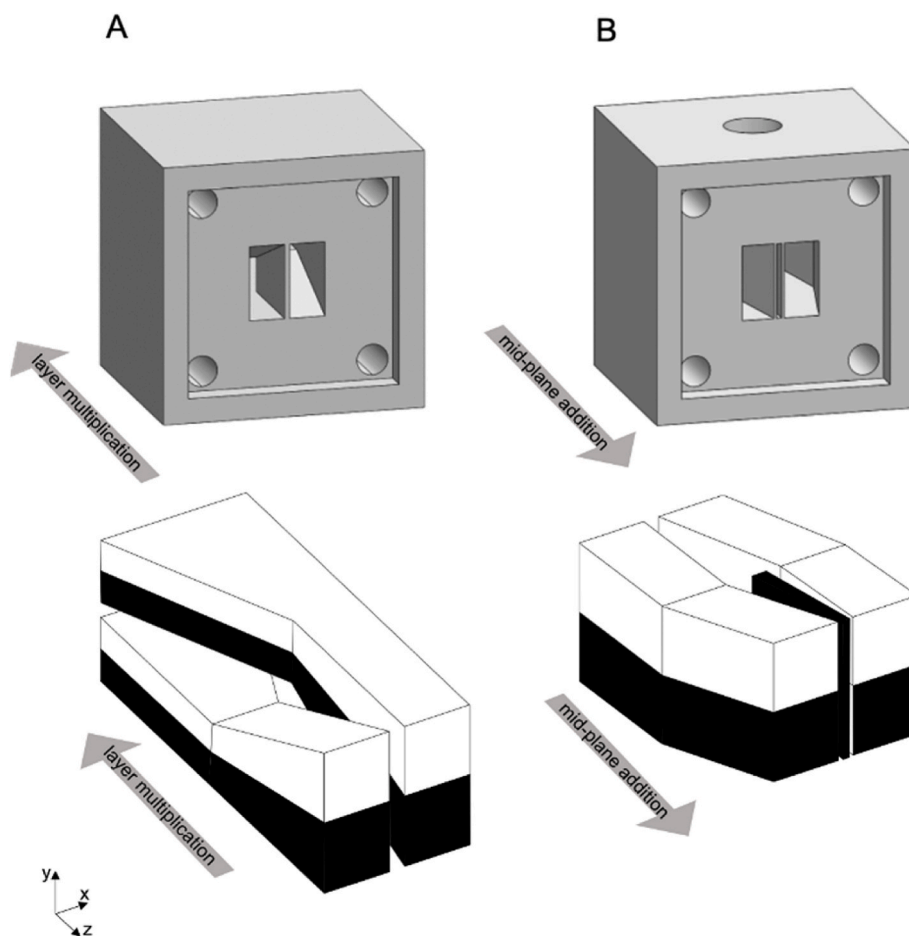


Fig. 4. Flow profile in Multiflux elements (A) splitting serpentine element for layer multiplication and (B) mid-plane addition element. Arrows indicate the direction of flow. Geometry adopted from (Neerinx et al., 2021).

elements, to improve layer thickness uniformity (van der Hoeven et al., 2001), (Fig. 5).

The tempered chocolates were filled into pre-heated stainless steel syringes connected to the Multiflux elements. The syringes were mounted in a Texture Analyzer Instron 5564 (Instron, USA) (Appendix Figure A2), which allowed to set a constant force and record the displacement over time. A constant force was set to 150 N to obtain volumetric flow rates, which resulted in a shear rate of 0.3 s^{-1} in the structuring channel. The channel was placed above a water bath of $40 \text{ }^\circ\text{C}$

to pre-heat the elements prior to structuring, and to avoid early solidification of the chocolate at the walls.

By adding two differently coloured dispersions to the Multiflux channel, 4, 8, 16, 32, 64, 128 and 256 layers were formed. The layer formation of the stained chocolate mixes was calculated with the following equation (1) (Neerinx et al., 2021):

$$b = 2^{n+1} \tag{1}$$

With b the number of resulting layers and n the number of layering

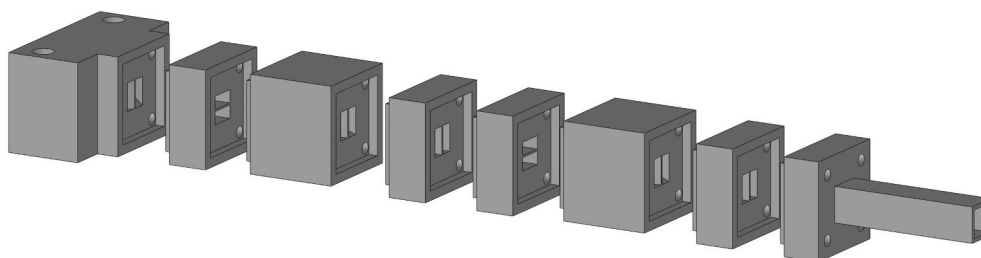


Fig. 5. From left to right the layer formation set-up contains the following elements: Feed (F), Pressure Homogenizer (H), Splitting Serpentine Mixer (S), Pressure Homogenizer (I), H, S, I, Outlet (O). The set-up was extended for up to seven Splitting Serpentine Mixers to obtain 256 layers, with a layer thickness of $\sim 60 \text{ }\mu\text{m}$.

operations. One layering operation results in 4 layers, two in 8 layers, three in 16 layers, up to seven, which gives 256 layers. With a channel width of 15 mm, the layer thickness after 7 folding operations corresponds to a theoretical layer thickness of approximately 60 μm . That is the maximum number of layers with which a layer thickness $>30 \mu\text{m}$ can be obtained. 30 μm is the limit for particle size above which the human palate can feel particles (Tiefenbacher, 2017), which we connect here to the layer thickness.

3.4.2. Wheat dough and melt cheese structuring

One stainless steel syringe was pre-heated for the melt-cheese sample, the other one was kept at room temperature. The pumps were connected to the Multiflux elements and a constant force of 1800 N was set, resulting in a shear rate of 0.02 s^{-1} . Due to the higher viscosities of the wheat dough and melt cheese, higher forces were necessary to push the materials through the channel. The set force was limited by the constraints from the texture analyzer, and this force did give lower low shear rate in case of this combination of materials compared to the shear rate obtained with chocolates.

The Multiflux elements were placed into the freezer after structure formation to shorten the solidification time of the chocolate and to fixate the structure of the wheat dough-melt cheese samples. Subsequently, structures were collected and cross sections were prepared through cutting. The structures were photographed with a Sony $\alpha 6000$ camera (Sony, Japan) equipped with a macrolens (Tokina, Japan), Fig. 8.

3.4.3. Formation of hierarchical structures with mid-plane additions

Hierarchical structures were formed by adding a mid-plane to the layered structures (Neerinx et al., 2021). Four splitting serpentine elements were combined with the pressure homogenizer elements to a channel to produce 16 layers, followed by the mid-plane addition element (Fig. 4) to form simple strand structures.

3.5. Rheological measurements

Rheological properties of the coloured chocolate, melt cheese and wheat dough were determined using the MCR-502 rheometer (Anton Paar GmbH, Graz, Austria). A cone-plate geometry ($\varnothing 50 \text{ mm}$, CP50-4) was used. The measurements were performed at increasing shear rates, set to increase from 0.1 s^{-1} - 100 s^{-1} (chocolate), or 0.001 s^{-1} - 10 s^{-1} (cheese and dough). The flow curves of the chocolate samples were obtained by plotting the shear stress (Pa) as a function of the shear rate (s^{-1}). It is assumed that the flow properties of the liquid chocolate samples ($40 \text{ }^\circ\text{C}$) that contain added pea fibre behave similar to those of liquid chocolate. Therefore, the viscosities and yield stresses were determined by fitting the Casson equation to the data (equation (2)) (De Graef et al., 2011). τ is the shear stress, τ_y the yield stress and η_c the Casson viscosity and $\dot{\gamma}$ the shear rate.

$$\sqrt{\tau} = \sqrt{\tau_y} + \sqrt{\eta_c \dot{\gamma}} \quad (2)$$

For wheat dough and melt cheese the viscosity was determined as a function of the shear rate at $25 \text{ }^\circ\text{C}$ and $40 \text{ }^\circ\text{C}$, respectively, according to the material temperature in the syringes. The viscosities of the materials were determined to compare the flow responses of the materials with each other to allow conclusions of their influence on the layer formation.

The apparent viscosity η of wheat dough and melt cheese was calculated at the respective shear rate in the channel, equation (3).

$$\eta = \frac{\tau}{\dot{\gamma}} \quad (3)$$

With τ the shear stress, and $\dot{\gamma}$ the shear rate.

3.6. Cutting tests

Uniaxial cutting of the structured chocolate samples was done with a Warner Bratzler rectangular slot blade (Stable Micro Systems, UK) in a TA. XT plusC Texture analyzer (Stable Micro Systems, UK) to determine the cutting force. The chocolate products were held at a temperature of $4 \text{ }^\circ\text{C}$ prior to testing. They were trimmed to a sample width and length of 15 mm and equal sample heights of 20 mm. The measurements were performed at room temperature and the blade was lowered at a constant velocity of 1 mm/s. The determined peak force from the tests was used, and compared for parallel and perpendicular cut chocolate samples.

4. Results

4.1. Formation of 256 layers with white and black stained chocolate mixes

Milk and white chocolate were stained with black and white cocoa butter, respectively for better distinction of the layers. The viscosities were adjusted with yellow pea fibre isolate. The viscosities of the black and white stained chocolate mixes were similar over a temperature decrease from 40 to $20 \text{ }^\circ\text{C}$ (Figure A 3). Hence, during cool down in the channel, they remained in the same range. The volumetric flow of the chocolate through the channel was approximately.

14 mL/min, which corresponded to a shear rate of around 0.5 s^{-1} . The viscosity of the chocolates and the shear stress on the chocolates was approximately the same in this range (Casson viscosity $\eta_{C,white} = 0.9 \text{ Pa s} \pm 0.1 \text{ Pa s}$, $\eta_{C,black} = 0.7 \text{ Pa s} \pm 0.2 \text{ Pa s}$, yield stresses $\tau_{y,white} = 10.8 \text{ Pa} \pm 2.4 \text{ Pa}$, $\tau_{y,black} = 11.6 \text{ Pa} \pm 1.2 \text{ Pa}$) (Figure A 3), and might thus not induce distortions during layer formation (Neerinx et al., 2021).

The layer formation of stained chocolate mixes in the Multiflux channel is depicted in Fig. 6. Mostly uniform straight layers were produced. The layers were still countable after five layering operations, thus 64 layers.

4.2. Structural anisotropy

The mechanical properties of the product were determined parallel and perpendicular to the layers. It was assumed that the layered structure would affect the material stiffness. The required force to cut the 8 layer and 16 layer structures was higher when cut perpendicular to the layers than that of parallel cut samples. Moreover, cutting the samples along the layers resulted in even breakage, which was not the case when cut perpendicular to the layers (Fig. 7). The peak cutting force was not determined for 4 layers, as the structures were too unstable and broke too quickly along the layer surfaces during cutting for sample preparation.

4.3. Layer formation with high viscosity dispersions

The structure formation in the Multiflux mixer was additionally tested with wheat dough and melt cheese to investigate if two different materials of higher viscosities could also be structured. While the melt cheese was heated for the experiments, the wheat dough was kept at room temperature. The apparent viscosity of the wheat dough and melt cheese was about a factor 10 higher than those of the chocolate (Appendix Figure A 4). Accordingly higher force was required to push the material through the channel (Section 3.4). The volumetric flow that could be achieved with the set-up was 0.7 mL/min. That also leads to a longer residence time of the material in the channel. The corresponding

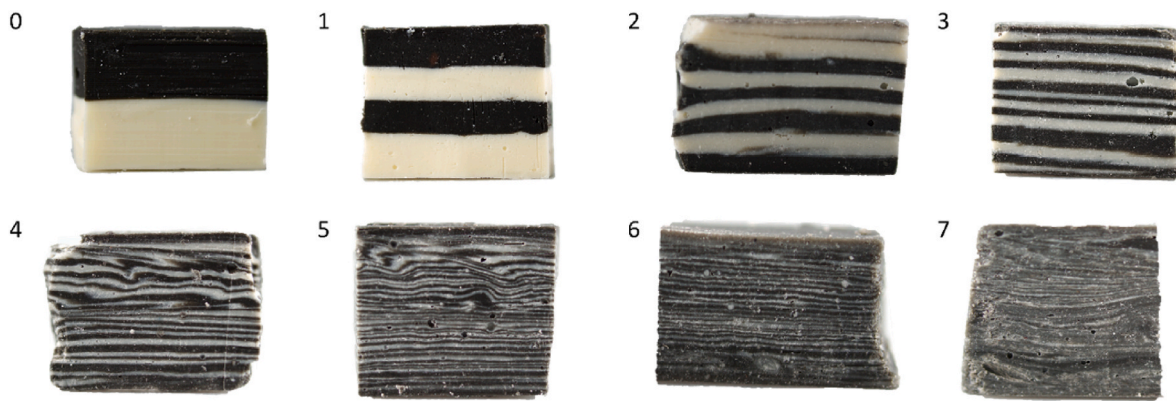


Fig. 6. Images of layer formation with stained milk chocolate and stained white chocolate. All samples have a height of 15 mm. (0) are the combined chocolates before the layering operations, (1) 1st layering operation, (2) 2nd layering operation, (3) 3rd layering operation, (4) 4th layering operation, (5) 5th layering operation, (6) 6th layering operation and (7) 7th layering operation.

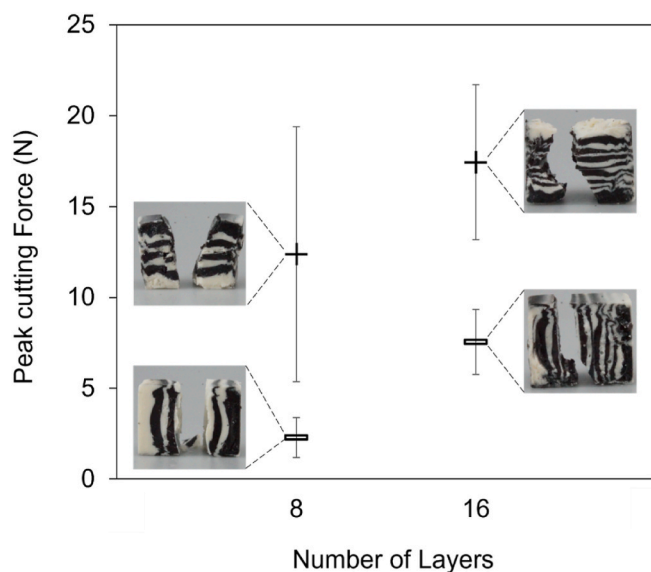


Fig. 7. The cutting force was measured as the peak force required to cut samples. The cutting force was determined for a structure of 8 layers, and 16 layers, with cuts parallel (≡) and perpendicular (+) to the layers. Cutting profiles are depicted in images next to the corresponding modulus, for a better comparison of the structures.

shear rate was calculated to be around 0.02 s^{-1} . Although, the viscosities profiles differed, and were of different magnitude at the respective shear rate (apparent viscosity $\eta_{cheese} = 39 \text{ MPa s} \pm 15 \text{ MPa s}$, $\eta_{dough} = 23 \text{ MPa s} \pm 4 \text{ MPa s}$), layers could be produced (Fig. 8). The cheese layer thickness was bigger than the dough layer thickness, possibly induced through differences in viscoelastic properties of the materials under stress (Appendix Figure A 4).

4.4. Factors influencing layer formation

For the structure formation with the splitting serpentine geometry, it has been previously described that matching viscosities are a prerequisite to produce uniform structures (Neerinx et al., 2021). To determine the range of viscosity dark, milk and white chocolate was used as a model material. All three varied in viscosity and shear stress over a shear rate of $0.1\text{--}100 \text{ s}^{-1}$, but followed similar viscosities curves (Appendix Figure A 3, A). At the corresponding shear rate in the structuring channel, layer formation of milk (Casson viscosity $\eta_{c,milk} = 0.6 \text{ Pa s} \pm 0.1 \text{ Pa s}$, yield stress, $\tau_{y,milk} = 12.0 \text{ Pa} \pm 0.4 \text{ Pa}$) and white chocolate ($\eta_{c,white} = 0.4 \text{ Pa s} \pm 0.0 \text{ Pa s}$, yield stress $\tau_{y,white} = 4.8 \text{ Pa} \pm 0.9 \text{ Pa}$) (Fig. 9 A), white ($\eta_{c,white} = 0.4 \text{ Pa s} \pm 0.0 \text{ Pa s}$) and dark chocolate ($\eta_{c,dark} = 7.6 \text{ Pa s} \pm 5.8 \text{ Pa s}$, $\tau_{y,milk} = 23.7 \text{ Pa} \pm 9.7 \text{ Pa}$) (Fig. 9 B), and milk ($\eta_{c,milk} = 0.1 \text{ Pa s} \pm 0.0 \text{ Pa s}$) and dark chocolate ($\eta_{c,dark} = 2.2 \text{ Pa s} \pm 1.6 \text{ Pa s}$) (Fig. 9 C) resulted in non-uniform layers, or distorted structures. Even though the Casson viscosities of the milk and white chocolate structures were



Fig. 8. Structured wheat dough and melt cheese into 0) 2 layers, 1) 4 layers, and 2) 8 layers. All samples have a height of 15 mm.

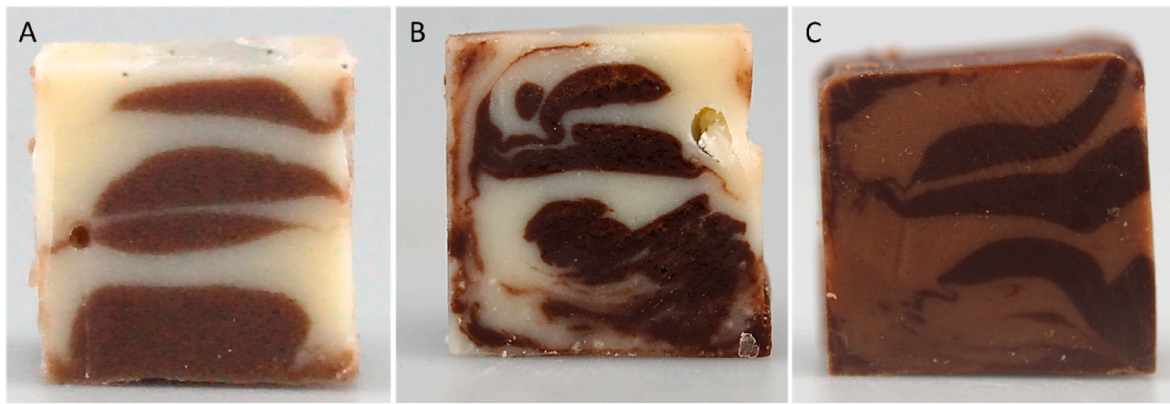


Fig. 9. Layer formation (8 layers) of (A) milk and white chocolate, (B) dark and white chocolate, and (C) dark and milk chocolate. All samples have a height of 15 mm.

relatively similar, the yield stresses (Appendix Figure A5) of the three chocolate samples were distinctly different, compared to those of the white and black stained chocolate samples (Appendix Figure A3 B). This underlines the importance of similar viscosity properties to avoid distortions. Hence, the similarity of the material viscosities is very relevant, while the magnitude of the material viscosity is less relevant, as uniform layers could be formed with the white and black stained chocolate samples, at relatively low Casson viscosities.

4.5. Structure formation of higher hierarchical level

A mid-plane addition element was added to the Multiflux channel to produce strands instead of layers (Fig. 4 A) (Neerinx et al., 2021). For the production of strands by a mid-plane addition, white and black stained chocolate, as well as melt cheese and wheat dough were used to see if both materials could produce similar structures. After the mid-plane addition in the chocolate samples, the tree structure described by Neerinx et al. (2021) were clearly observable, and all 16 branches could be observed (Fig. 10 B). However, the branches were slightly bended towards the middle from both sides. Mid-plane addition in the cheese dough sample resulted in a more distorted structure. The mid-addition is clearly present, while the branches are even more bended. Due to the distortions not all 16 expected branches were visible. Neerinx et al. (2021) pointed out that these distortions are a result of

normal stress differences in viscoelastic fluids, or differences in viscosities.

The distortions of the ‘branches’ in the cheese-dough sample could be additionally induced through the elastic properties of the dough phase that formed wavy structures upon relaxation. The results in Section 4.4 already highlighted the importance of similar viscosities for layer formation. Here, it becomes obvious that in order to create hierarchical structures similar viscosities are even more important, as evidenced by the fact that the cheese dough structures are more distorted. Furthermore, the bended branches of the chocolate sample indicate that formation of hierarchical structure is even more difficult, as these distortions will likely enhance with subsequent hierarchy increases. The structures obtained by Neerinx et al. (2021) with black and white stained Nivea cream samples, were more uniform at slightly higher viscosities of 50 Pa and similar viscosity profiles. The lesser uniformity of the chocolate structure might be a result of the crystallization properties of the chocolate samples that could occur at the geometry wall, due to cool down of the geometry and material during structuring.

5. Discussion

The layer and structure formation via this laminar fractal structuring process seems a promising process for various food applications to produce layers or strand-like structures. We could show with our



Fig. 10. The structure design (A) to produce a tree structure from 16 layers through a mid-plane addition, adapted from (Neerinx et al., 2021) and the experimental results with (B) white and black stained chocolate, and (C) melt cheese and wheat dough. (A and B) Depict the structure after one mid-plane addition, (C and D) depict the structure after a subsequent layering operation. Both samples have a height of 15 mm.



Fig. 11. Cross section of four layer melt cheese sample, showing alignment of dill leaf in flow direction. The sample has a height of 15 mm.

experiments that food dispersions of varying but matching viscosities can be layered in the Multiflux channel. The structure formation with the wheat dough and melt cheese was restricted by the maximum force of the experimental set-up. Schaller et al. (2017) connected the Multiflux channel to two single-screw extruders to process polystyrene and amorphous polyamide at high temperatures (200 °C and 270 °C, respectively). A similar set-up here would allow to push higher viscosity dispersion through the channel and extend the possibilities to apply the method for foods.

The method offers additionally the potential to structure food dispersions on a substructure level. The convergence of the structuring channel to induce stretching of the fluid has the additional effect of component orientation in the stream. When polymer chains, such as proteins are exposed to an extensional flow for a sufficient amount of time or distance, those polymer chains can stretch and orient in the fluid (Hsiao et al., 2017; Rivlin, 1948). Such an alignment could induce an additional fibre formation in the food dispersion on a microscale. Protein alignment in food dispersions occurs for example in Mozzarella cheese kneading, i.e. oriented casein micelle chains. Fibre formation on different length scales, strands on macroscale, and oriented and stretched molecule chains on microscale could result in enhanced anisotropy. Such structural levels could add to the elasticity and texture of the strands and hence to the textural properties of food.

In order to understand if an orientation in the direction of flow could be achieved in the Multiflux channel, even at the conditions tested in this research, dill leaves were added to melt cheese. The dill leaves were only added to one syringe filled with melted cheese and up to four layers were formed. Indeed, orientation in the direction of flow could be visualized by orienting a dill leaf in a four layer melt cheese sample (Fig. 11). This indicates that anisotropy can be induced also within the layers, through orientation in the direction of flow at the length scale of the dill leaf. Different channel geometries could be studied in a computer simulation at varying viscosities and volume flow conditions using models as proposed by (Jaspe and Hagen, 2006) to understand which level of molecular aggregation is required to create orientation under flow conditions present in such structuring channels.

The continuity of the process, as well as its scalability makes it

attractive for the production of a variety of food products. These include layered pastry, or novel chocolate structures, such as presented above. Layers can provide texture experiences, and allow the combination of materials with different flavour profiles, e.g. differences in sweetness or saltiness (Kistler et al., 2021). Furthermore, the strand formation in combination with the potential orientation of food proteins has potential to produce novel food structures with anisotropy at different length scales.

6. Conclusions

The static Multiflux mixer allowed the formation of stratified structures with food materials. The materials, which resulted in the most homogeneous layers after only two layer duplications were used to produce up to 256 layers of an estimated layer thickness of 60 µm. Chocolate served as a model material, due to its melting and solidification properties at intermediate temperatures. Layer formation with higher viscosity materials, such as wheat dough and melt cheese, could also be achieved. The presence of layer in chocolate-based product resulted in anisotropy in the mechanical properties. The required cutting force was lower when the product was cut in parallel direction, than when it was cut perpendicular to the layers. Probably, additional anisotropy can be induced in the structures in each layer as indicated by the oriented dill leaf in the direction of flow. The application of higher forces could open even new opportunities for structure formation, i.e. easing the fixation of the structures, and investigating the potential to induce orientation at smaller length scale in protein-rich dispersions.

Credit author statement

Anna Cäcilie Möller: Conceptualization, Methodology, Data curation, Formal analysis, Investigation, Validation, Visualization, Writing – original draft. Albert van der Padt: Conceptualization, Validation, Writing – review & editing, Supervision, Project administration. Atze Jan van der Goot: Conceptualization, Validation, Writing – review & editing, Supervision.

Declaration of competing interest

The authors declare that they have no known competing financial interests or personal relationships that could have appeared to influence the work reported in this paper.

Data availability

Data will be made available on request.

Acknowledgements

The authors would like to thank Andre Sanders for his inspiration and enthusiasm to build the structuring set-up. The authors would like to thank Prof. Dr Han Meijer for valuable insight and stimulating discussions. This research took place within the framework of the Institute of Sustainable Process Technology and is co-funded by TKI-Energy with the supplementary grant ‘TKI-Toeslag’ for Topconsortia for Knowledge and Innovation (TKI’s) of the Ministry of Economic Affairs and Climate Policy.

Appendix

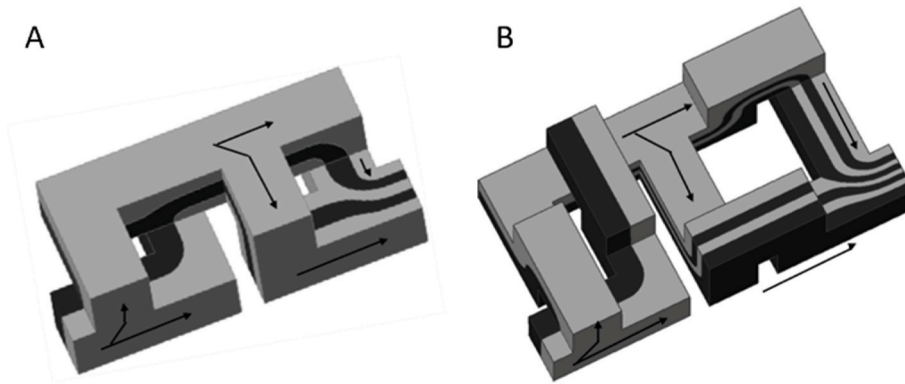


Fig. A1. The Chen mixer (A) makes use of the stretching-folding operation, the Dentincx mixer (B) makes use of the stretching-stacking operation. Both mixers include interface rotation to reorient layers parallel to each other for layer multiplication. Images reprinted with permission (Schaller et al., 2017).



Fig. A2. Syringe pump set-up mounted in Texture analyzer.

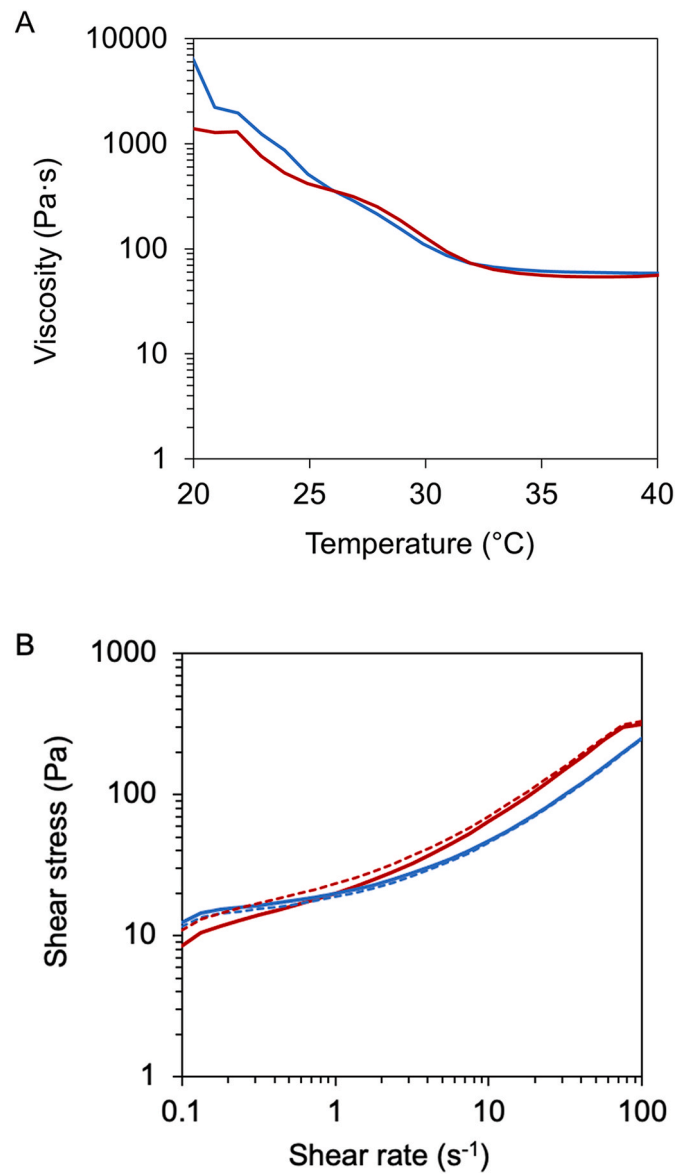


Fig. A3. Viscosity of black — and white — stained chocolate mixes (A) over a temperature ramp from 40 °C to 20 °C, (B) shear stress against shear rate at 40 °C. Broken lines represent the Casson fit at the respective viscosities and yield stresses. Viscoelastic properties were determined in duplicate and a representative curve was selected.

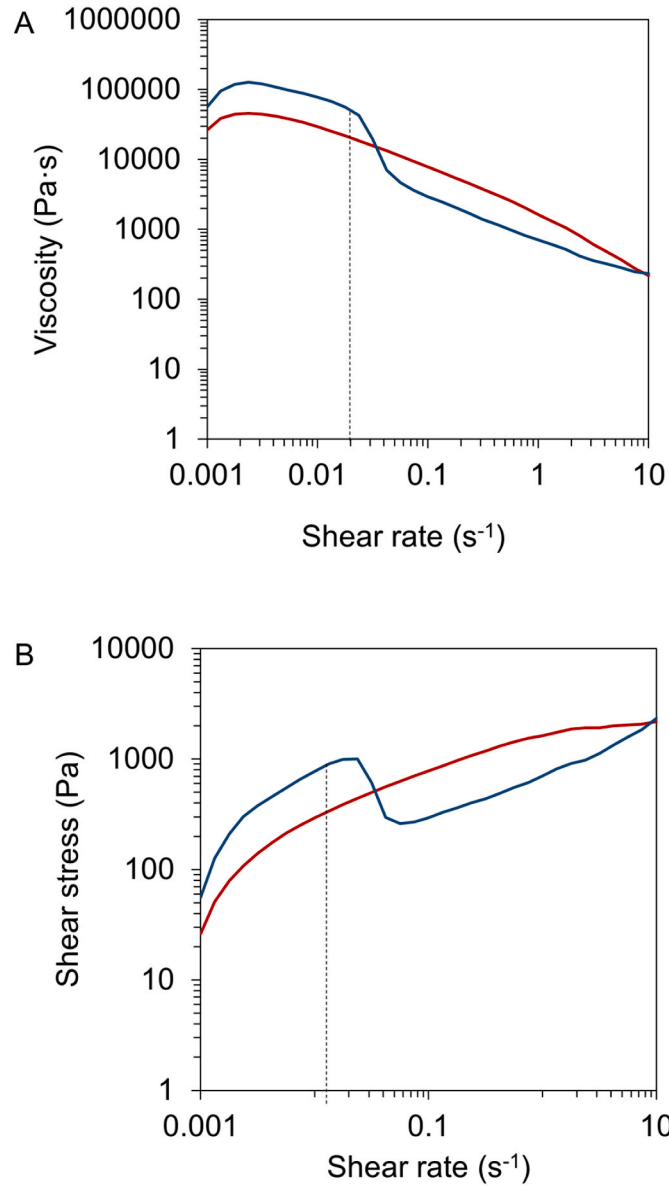


Fig. A4. Viscosity of wheat dough — at 25 °C and melt cheese — at 40 °C at increasing shear rates. Shear stress plotted against shear rate for the same samples (B). Viscoelastic properties were determined in duplicate and a representative curve was selected..

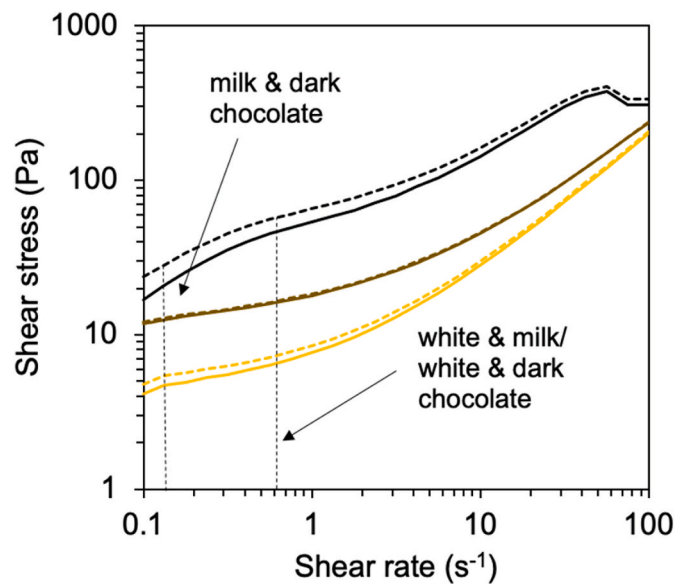


Fig. A5. Shear stress against shear rate depicted for dark —, milk — and white — chocolate. Respective shear rates are marked (dotted lines). Broken lines represent the Casson fit at the respective viscosities and yield stresses. Viscoelastic properties were determined in duplicate and a representative curve was selected.

References

- Cappelli, A., Bettaccini, L., Cini, E., 2020. The kneading process: a systematic review of the effects on dough rheology and resulting bread characteristics, including improvement strategies. *Trends Food Sci. Technol.* 104 (August), 91–101. <https://doi.org/10.1016/j.tifs.2020.08.008>.
- De Graef, V., Depypere, F., Minnaert, M., Dewettinck, K., 2011. Chocolate yield stress as measured by oscillatory rheology. *Food Res. Int.* 44 (9), 2660–2665. <https://doi.org/10.1016/j.foodres.2011.05.009>.
- Hofmann, M., Bayles, A.V., Vermant, J., 2021. Stretch, fold, and break: intensification of emulsification of high viscosity ratio systems by fractal mixers. *AIChE J.* 67 (5) <https://doi.org/10.1002/aic.17192>.
- Hsiao, K.-W., Sasmal, C., Ravi Prakash, J., Schroeder, C.M., 2017. Direct observation of DNA dynamics in semidilute solutions in extensional flow. *J. Rheol.* 61 (1), 151–167. <https://doi.org/10.1122/1.4972236>.
- Jaspe, J., Hagen, S.J., 2006. Do protein molecules unfold in a simple shear flow? *Biophys. J.* 91 (9), 3415–3424. <https://doi.org/10.1529/biophysj.106.089367>.
- Kistler, T., Pridal, A., Bourcet, C., Denkel, C., 2021. Modulation of sweetness perception in confectionary applications. *Food Qual. Prefer.* 88, 104087 <https://doi.org/10.1016/j.foodqual.2020.104087>.
- Kugler, S.K., Dey, A.P., Saad, S., Cruz, C., Kech, A., Osswald, T., 2020. A flow-dependent fiber orientation model. *Journal of Composites Science* 4 (3), 1–22. <https://doi.org/10.3390/jcs4030096>.
- Lillford, P.J., 2016. The impact of food structure on taste and digestibility. *Food Funct.* 7 (10), 4131–4136. <https://doi.org/10.1039/c5fo01375e>.
- Liu, Z., Zhang, M., Bhandari, B., Wang, Y., 2017. 3D printing: printing precision and application in food sector. *Trends Food Sci. Technol.* 69, 83–94. <https://doi.org/10.1016/j.tifs.2017.08.018>.
- Ma, Y., Schutyser, M.A.I., Boom, R.M., Zhang, L., 2021. Predicting the extrudability of complex food materials during 3D printing based on image analysis and gray-box data-driven modelling. *Innovat. Food Sci. Emerg. Technol.* 73 (April), 102764 <https://doi.org/10.1016/j.ifset.2021.102764>.
- McMahon, D.J., Fife, R.L., Oberg, C.J., 1999. Water partitioning in Mozzarella cheese and its relationship to cheese meltability. *J. Dairy Sci.* 82 (7), 1361–1369. [https://doi.org/10.3168/jds.S0022-0302\(99\)75361-0](https://doi.org/10.3168/jds.S0022-0302(99)75361-0).
- Muscalu, G., Voicu, G., Istudor, A., Tudor, P., 2020. Bread dough rheological behavior under the influence of the geometry of the kneading arms. *Rev. Chem.* 70 (9), 295–307. <https://doi.org/10.37358/RC.20.9.8340>.
- Nachal, N., Moses, J.A., Karthik, P., Anandharamakrishnan, C., 2019. Applications of 3D printing in food processing. *Food Eng. Rev.* 11 (3), 123–141. <https://doi.org/10.1007/s12393-019-09199-8>.
- Neerinx, P.E., Denteneer, R.P.J., Meijer, H.E.H., 2011a. A fully polymeric mouldable microfluidic device. Part 1: the process of design. *Macromol. Mater. Eng.* 296 (12), 1081–1090. <https://doi.org/10.1002/mame.201100047>.
- Neerinx, P.E., Hellenbrand, S.J.M., Meijer, H.E.H., 2011b. A fully polymeric mouldable microfluidic device. Part 2: designing the process. *Macromol. Mater. Eng.* 296 (12), 1091–1100. <https://doi.org/10.1002/mame.201100048>.
- Neerinx, P.E., Hofmann, M., Gorodetskyi, O., Feldman, K., Vermant, J., Meijer, H.E.H., 2021. One-step creation of hierarchical fractal structures. *Polym. Eng. Sci.* 61 (4), 1257–1269. <https://doi.org/10.1002/pen.25677>.
- Neerinx, P.E., Meijer, H.E.H., 2013. Fractal structuring in polymer processing. *Macromol. Chem. Phys.* 214 (2), 188–202. <https://doi.org/10.1002/macp.201200394>.
- Pietsch, V.L., Karbstein, H.P., Emin, M.A., 2018. Kinetics of wheat gluten polymerization at extrusion-like conditions relevant for the production of meat analog products. *Food Hydrocolloids* 85 (July), 102–109. <https://doi.org/10.1016/j.foodhyd.2018.07.008>.
- Rivlin, R.S., 1948. Normal stress coefficient in solutions of macromolecules. *Nature* 161 (4093), 567–568.
- Sandoval Murillo, J.L., Osen, R., Hiermaier, S., Ganzenmüller, G., 2019. Towards understanding the mechanism of fibrous texture formation during high-moisture extrusion of meat substitutes. *J. Food Eng.* 242, 8–20. <https://doi.org/10.1016/j.jfoodeng.2018.08.009>. August 2018.
- Schaller, R., Neerinx, P.E., Meijer, H.E.H., 2017. Hierarchical and fractal structuring in polymer processing. *Macromol. Mater. Eng.* 302 (6), 1–14. <https://doi.org/10.1002/mame.201600524>.
- Tiefenbacher, K.F., 2017. Adjuncts—filling creams, inclusions, cacao and chocolate. In: *Wafer and Waffle*. <https://doi.org/10.1016/b978-0-12-809438-9.00005-3>.
- van der Hoeven, J.C., Wimbergen-Friedl, R., Meijer, H.E.H., 2001. Homogeneity of multilayers produced with a static mixer. *Polym. Eng. Sci.* 41 (1).
- Vincent, M., Agassant, J.F., 1985. Experimental and theoretical study of short fiber orientation in diverging flows. *Rheol. Acta* 24 (6), 603–610. <https://doi.org/10.1007/BF01332594>.